Research on Magnetic Resonance Imaging Segmentation Algorithm

Lin Chen, Dong Wei *, and Jie-Sheng Wang *

Abstract—**Magnetic resonance imaging (MRI) has become an important auxiliary means in the clinical diagnosis of brain diseases and other diseases. The brain images segmentation based on MRI technique mainly includes the segmentation of normal brain tissues and brain images with lesions. The gray-scale distribution of MRI brain images is not uniform because of the noise, migration field effect and partial volume effect in the process of producing the MRI images, and the performance under different image segmentation algorithms is different. The segmentation experiments on single tissue images, MRI brain images and brain abnormal tissue images were carried out based on seven segmentation algorithms (level set, cross entropy, fuzzy entropy, maximum between-class variance, expectation maximization, k-means clustering and fuzzy c-means clustering). The simulation results compared the performance of these seven image segmentation algorithms on the typical MRI brain images.**

Index Terms—**Magnetic resonance imaging, Segmentation algorithm, Performance comparison**

I. INTRODUCTION

MAGNETIC resonance imaging (MRI) is a technique to produce the reconstructed images by adopting the signals produced by the nucleus in a magnetic field. After radio frequency pulses are applied outside the human body, the hydrogen atoms in the human body absorb the energy from these radio frequency pulses and produce an MRI that reaches the excited state. After the radio frequency pulse stops, the human hydrogen atoms return to their original state. Magnetic resonance signals are produced during this process. As a result, MRI does a very good effect of imaging the soft tissues of the brain that are rich in hydrogen atoms. As an important imaging technology in the field of medical imaging technology, MRI has been widely used in the diagnosis of human tissues and organs anatomy, pathological observation and other aspects due to its high-quality imaging effect and the advantages of easy observation of tissue structure [1]. Because MRI has good contrast between normal and pathological soft tissue, the main application is to dissect and observe the brain tissue structure and the diagnosis of brain pathological tissue.

Medical image segmentation, as an early processing technology for other medical image processing and pattern recognition, such as three-dimensional reconstruction and feature quantification, can provide strong support on the auxiliary diagnosis and treatment, clinical diagnosis and medical research. However, the development of imaging technology is not enough to realize the aspiration of the above auxiliary medical functions. It is necessary to meet the requirements of imaging technology or equipment for rapid and accurate segmentation of the generated medical images, which is an important technology in the field of late-stage medical image processing at present. In the process of image processing, different segmentation methods should be selected according to different medical images.

Image segmentation is to divide the image into several specific and unique regions, which have similar properties, such as gray, color, texture, brightness, contrast, etc. When the MRI image is segmented, the segmentation effect is different for different positions or layers [2]. In the segmentation analysis of a large number of image data, it is necessary to determine the image type with segmentation, and select the appropriate segmentation method according to the specific imaging type. In addition, in the actual work, the manufacturing process and external environment noise will lead to the partial distortion of the original data, which will have a certain impact on image compression and segmentation. Therefore, how to accurately segment these brain images on the basis of preserving the original images to the maximum extent has become the focus of current research in the medical image processing field.

At present, the commonly used medical image segmentation methods mainly include the regional-based segmentation methods, the edge-based segmentation methods, the horizontal set-based segmentation methods, the neural network based segmentation methods, the fuzzy theory based segmentation methods and the wavelet transform based segmentation methods, etc [3]. Among them, the region-based segmentation methods include threshold method, region growth and division combination, classifier and cluster, and random airport-based methods [4-6]. Segmentation method based on edge is in that the changes of the pixel gray values on the edge of the area tend to be more severe, so the edge between different regions is adopted to solve the image segmentation problem, which includes the parallel differential operator method, the curved surface fitting method, the method based on boundary curve fitting,

Manuscript received January 21, 2019; revised April 11, 2019. This work was supported by the Basic Scientific Research Project of Institution of Higher Learning of Liaoning Province (Grant No. 2017FWDF10), and the Project by Liaoning Provincial Natural Science Foundation of China (Grant No. 20180550700).

Lin Chen is with the School of Electronic and Information Engineering, University of Science and Technology Liaoning, Anshan, 114051, PR China (e-mail: EDMM888888@163.com).

Dong Wei is with the School of Electronic and Information Engineering, University of Science and Technology Liaoning, Anshan, 114051, PR China. (Corresponding author, phone: 86-0412-5929747; fax: 86-0412-2538244; e-mail: asweidong@126.com.

Jie-Sheng Wang is with the School of Electronic and Information Engineering, University of Science and Technology Liaoning, Anshan, 114051, PR China; National Financial Security and System Equipment Engineering Research Center, University of Science and Technology Liaoning. (Corresponding author, phone: 86-0412-2538355; fax: 86-0412-2538244; e-mail: wang_jiesheng@126.com).

serial boundary search as well as the method based on deformation model [7-8]. The segmentation method based on the horizontal set is a segmentation method based on the geometric deformation model. The evolution problem of a closed curved flexible surface in two or three dimensions is transformed into an implicit method for the evolution of a level set function curved surface in a high dimensional space [9-10]. The segmentation algorithm based on neural network is to realize the pattern classification on the medical image segmentation through the artificial neural network. According to the topology, the neural network technology can be divided into forward neural network, feedback neural network and self-organizing mapping neural network [11-13]. The segmentation method based on fuzzy theory adopts the fuzzy theory to realize the fuzzy clustering on the target images, which is suitable for image segmentation of images with features of uncertainty and ambiguity [14-16]. The segmentation method based on wavelet transform divides the image histogram into wavelet coefficients with different levels by using binary wavelet transforms. The threshold is selected according to the given segmentation criteria and wavelet coefficients. The whole process is from coarse to fine, and is controlled by scale [17].

The segmentation of MRI brain images mainly includes the segmentation of normal brain tissue and MRI brain images with lesions. Due to the influence of noise, migration field effect and partial volume effect in MRI images, the gray scale distribution of MRI brain images is not uniform, and the performance of different image segmentation algorithms is different. The thesis of single tissue images segmentation, brain MRI images and brain abnormal tissue images were carried out based on seven segmentation algorithms (level set, cross entropy, fuzzy entropy, maximum between-class variance, expectation maximization, k-means clustering and fuzzy c-means clustering). The simulation results are compared and the differences among the methods are analyzed to verify the effectiveness of the adopted segmentation algorithms.

II. IMAGE SEGMENTATION ALGORITHMS

A. Concept of Image Segmentation

In the study and application of images, some parts of the image are usually only interested, which are usually named as foreground or target and the rest are called background. The target usually corresponds to specific and unique regions in the image, which can be the gray value of the pixel, edge contour curve of the stage, color or texture, etc. Image segmentation is the technology and procedure to divide the image into various regions with characteristics and extract the interested objects. The definition of the image segmentation can be described as follows. Let the set R represent the whole image region, and the segmentation of R can be regarded as decomposing R into N non-empty sets R_1, R_2, …, R_N, which satisfies:

a. $\bigcup_{i=1}^{N} R_i = R$;

b. For all i and j, when $i \neq j$, satisfy $R_i \cap R_j = \emptyset$;

c. For $i = 1,2,\cdots,N$, there is $P(R_i) = \text{TRUE}$;

d. For $i \neq j$, there is $P(R_i \cup R_j) = \text{FALSE}$;

e. For $i = 1,2,\cdots,N$, R_i is the connected region.

where, P is the logical predicate for all the elements in the R_i set, and Ø represents an empty set.

According to the above definition, there are five conditions in the segmentation on an image. (1) The union set of all sub-regions obtained by the segmentation method should include all pixels in the image. In other word, the segmentation should divide every pixel in the image into a certain sub region. (2) Each sub region in the segmentation results is non-overlapping. That is to say, each pixel cannot simultaneously belong to different regions. (3) The obtained pixels belonging to the same region after segmentation should have some same characteristics. (4) The pixels in different regions obtained after further segmentation have some different characteristics. (5) The pixels in the same sub region in the segmentation results should be connected.

Image segmentation plays an important role in image processing engineering. It is a key step from image processioning to image recognition and understanding. The original images, such as image segmentation, target expression based on segmentation, feature extraction and parameter measurement, are transformed into more abstract and compact forms, which will make it possible to recognize, analyze and understand the higher level characteristic on images. Image segmentation is very important in many fields. At present, especially medical image segmentation is of great significance in human anatomy, clinical diagnosis, pathological analysis and treatment detection.

B. Classification of Image Segmentation Algorithms

There are many image segmentation methods, which mainly can be divided into the statistical segmentation method, the threshold-based segmentation method, the edge-based segmentation method, the region-based segmentation method and the fuzzy theory-based segmentation method.

(1) The segmentation method based on statistics. The essence of this method is to model the digital image from the perspective of statistics, regard the gray value of each pixel in the image as a random variable with a certain probability distribution, and gradually recover to the actual object or accurately segment the observed image from the observed image. The common statistical segmentation methods include classifier and clustering, hybrid distribution, image segmentation based on random field, and Hidden Markov models (HMM).

(2) Threshold-based segmentation method. Because the feature of image processing is intuitive and easy to implement and the threshold segmentation can always define non-overlapping regions with the closed and connected boundaries, it is especially suitable for images with different gray scale grades occupied by objects and backgrounds. This kind of methods can be divided into the global threshold and the local threshold.

(3) Edge-based segmentation method. The gray value of the pixel at the edge of the image is discontinuous, which can be detected by taking the derivative. For the step-edge, its position corresponds to the extreme value of the first derivative and the zero-crossing point of the second derivative (also called the zero-crossing point). The commonly used first-order differential operators are Roberts operator, Prewitt operator and Sobel operator. The commonly used second-order differential operators include Laplace operator, Kirsh operator and so on.

(4) Region-based segmentation method. A pixel cannot be separated from a target and judged solely on its gray scale value (e.g. the intensity-based method). They combine measures of pixel continuity to determine whether these pixels belong to the same region (or target).The region-based segmentation methods mainly includes the region growth method and the region splitting and merging method, which are two typical serial region technologies. The processing of the subsequent steps of the segmentation process should be judged according to the results of the previous steps.

(5) Fuzzy theory-based segmentation method. Image segmentation is a problem with poor structure to some extent, and fuzzy set theory just has the ability to describe this problem. The segmentation techniques based on fuzzy theory include the fuzzy threshold, the fuzzy clustering and the fuzzy edge detection.

C. Typical Image Segmentation Methods

1. Level Set

The level set method based on the set deformation model was first proposed in 1988, which is used to describe the structural changes with high dynamics and high topology, such as the boundary of combustion flames. The level set method adopts the high-dimensional function curved surface to express the evolution of the low dimensional curve or surface. The zero level set of the level set function is adopted to describe the curve or surface (interface), then the evolution equations of the curve or surface are transformed into the evolution partial differential equations of the higher dimensional level set function. By solving equations of the level set function, the movement boundary surface can be captured. On the other hand, the method can be easily extended to the arbitrary dimension.

The standard level set can be defined as follows. The level set of the differentiation function f: $R^n \to R$ in accordance to the real value C is the real point set $\{(x_1,x_2,\cdots,x_n)|f(x_1,x_2,\cdots,x_n) = C\}$, which is named as the differentiate function and f is the level set function.

Suppose the implicit function $\varphi(x,t)$ represent a high-dimensional space equation and the contact area in the low dimensional space $\varphi(x,t) = 0$, where $x = (x_1,x_2,\cdots,x_n) \in R^n$. So, the level set can be expressed as $\Gamma(t)$, which has the following properties: (1) $\varphi(x,t) < 0$ for $x \in \Omega$; (2) $\varphi(x,t) > 0$ for $x \notin \Omega$; (3) $\varphi(x,t) = 0$ for $x \in \partial\Omega = \Gamma(t)$.

Based on the above definition, the mathematical explanation of the level set method can be expressed as: the curve $\Gamma(t)$ along the found direction can be implicitly described as the zero level set function with a higher dimension.

$$\Gamma(t) = \{x|\varphi(x(t),t) = 0\} \tag{1}$$

Calculate the derivative on both sides of Eq. (1) with respect to time *t*, so obtain:

$$\varphi_t + \nabla\varphi(x(t),t) \cdot x'(t) = 0 \tag{2}$$

The curve is moving along its normal direction, so the force direction of each point on the curve can be viewed as along the outer normal direction. It can be known that $x'(t) \cdot n = F$ and the unit normal vector $n = \frac{\nabla\varphi}{|\nabla\varphi|}$. Then Eq. (2) can be expressed as:

$$\varphi_t + F|\nabla\varphi| = 0 \tag{3}$$

Eq. (3) is the level set equation. It can be seen that in the process of image segmentation, F is related to the information contained in the image itself and the curve $\varphi(t)$ in the application. For solving the above equation, the time finite-difference method is usually adopted, that is to say:

$$\frac{\varphi^{t+\Delta t}-\varphi^t}{\Delta t} = F|\nabla\varphi| \tag{4}$$

When considering the three-dimensional image domain, obtain:

$$\nabla\varphi = \left[\frac{\partial\varphi}{\partial x},\frac{\partial\varphi}{\partial y},\frac{\partial\varphi}{\partial z}\right] \tag{5}$$

$$|\nabla\varphi| = \sqrt{\left(\frac{\partial\varphi}{\partial x}\right)^2 + \left(\frac{\partial\varphi}{\partial y}\right)^2 + \left(\frac{\partial\varphi}{\partial z}\right)^2} \tag{6}$$

In general, $\varphi(x(t),t = 0) = \pm d$, where $\pm$ d is the symbol distance between the point in the image domain and the closed curve (curved surface). In general, if $\pm$ d is inside the curve (curved surface), take the negative. If $\pm$ d is outside the curve (curved surface), take the positive.

Step 1: Calculate the velocity *F* and the modulus of the gradient $|\nabla|\varphi$.

Step 2: Substitute the calculated φ^t,F,$|\nabla\varphi|$ into Eq. (3)-(4) to obtain $\varphi^{t+\Delta t}$.

Step 3: Find the zero level set function again. Reinitialize to make the each point in the image domain have the symbol distance function about the zero level set function.

Step 4: Judge the convergence. If realizing the convergence, stop the iteration. Otherwise, continue the iteration process, that is to say repeat from Step 1 to Step 4 until reach the convergence and stop the iteration.

2. Cross Entropy

Cross entropy is an important concept in Shannon information theory, which is used to measure the difference information between two probability components. The simple meaning of cross entropy is the difficulty of identifying text using the model. In the information theory, Cross entropy represents two probability distributions *p* and *q*, where *p* represents the real distribution and *q* represents the non-real distribution. *p* is used to measure the expectation of the coding length needed to identify a sample, which is represented as:

$$H(p) = \sum_i p(i) \cdot \log\left(\frac{1}{p(i)}\right) \tag{7}$$

However, if the non-real distribution *q* is used to represent the average coding length from the real distribution *p*, it should be represented as:

$$H(p,\ q) = \sum_i p(i) \cdot \log\left(\frac{1}{q(i)}\right) \tag{8}$$

Then $H(p,\ q)$ is named as cross entropy. The specific calculation method is described as follows.

(1) For the discrete variables, $\mathrm{H}(p, q) = \sum_x p(x) \cdot \log\left(\frac{1}{q(x)}\right)$.

(2) For the continuous variables, $-\int_X p(x)\log Q(x)dr(x) = E_p[-\log Q]$.

3. Fuzzy Entropy

As well as the physical meaning of approximate entropy (AE) and sample entropy (SE), fuzzy entropy (FE) also measures the generation probability of the new mode. When the measured value is larger, the generation probability of new mode is larger, that is to say that the sequence complexity is larger. The specific mathematical algorithm of fuzzy entropy (FE) is described as follows.

Step 1: For an *M*-point sampling sequence $\{u(j){:}1 \le j \le M\}$.

Step 2: Reconstruct a set of *n*-dimensional vectors in order of sequential order:

$$X_j^m = \{u(j),u(j+1),\cdots,u(j+n-1)\} - u_0(j) \quad (j = 1,\cdots,M-n) \tag{9}$$

where, $\{u(j),u(j+1),\cdots,u(j+n-1)\}$ represents the value of *n* consecutive *u* starting from the *j*-th point, and $u_0(j)$ represents the mean value, which is described as:

$$u_0(j) = \frac{1}{n}\sum_{i=0}^{n-1} u(i+j) \tag{10}$$

Step 3: The distance d_{ij}^n between the two *n*-dimensional vectors X_i^n and X_j^n is defined as the maximum difference between the corresponding elements.

$$d_{ij}^n = \mathrm{d}\left[X_i^n, X_j^n\right] = \max_{k\in(0,n-1)} \{|u(j+k) - u_0(j) - (u(i+k) - u_0(i))|\}\ (i,j = 1,\cdots M-n, i \ne j) \tag{11}$$

Step 4: The similarity D_{ij}^n between two vectors X_i^n and X_j^n is defined by using the fuzzy function $\mu\left(d_{ij}^n,m,r\right)$.

$$D_{ij}^n = \mu\left(d_{ij}^n,m,r\right) = exp\left(\left(-d_{ij}^n\right)^m / r\right) \tag{12}$$

where, function $\mu\left(d_{ij}^n,m,r\right)$ is an exponential function, *m* and *r* are the gradient and width of exponential function boundary, respectively.

Step 5: Define the following function:

$$O^n(\mathrm{m,r}) = \frac{1}{M-n}\sum_{i=1}^{M-n}\left\{\frac{1}{M-n-1}\sum_{j=1,i\ne j}^{M-n} D_{ij}^n\right\} \tag{13}$$

Step 6: Repeat Step 2 to 5 so as to reconstruct a group of *n*+1 dimensional vectors, which can be defined as:

$$O^{n+1}(\mathrm{m,r}) = \frac{1}{M-n}\sum_{i=1}^{M-n}\left\{\frac{1}{M-n-1}\sum_{j=1,i\ne j}^{M-n} D_{ij}^{n+1}\right\} \tag{14}$$

Step 7: Then the fuzzy entropy can be defined as:

$$\mathrm{FuzzyEn}(n,m,r) = \lim_{M\to\infty}\left[\ln O^n(m,r) - \ln O^{n+1}(m,r)\right] \tag{15}$$

When *M* value is finite, the estimated value of fuzzy entropy with serial number length *M* can be calculated by:

$$\mathrm{FuzzyEn}(n,m,r,N) = \ln O^m(m,r) - \ln O^{m+1}(m,r) \tag{16}$$

4. Maximum Between-Class Variance Method

Maximum between-class variance method (Otsu's method) is derived from the least square method, whose basic idea is to use a certain gray level as a threshold to divide the histogram of an image into two groups and calculate the variance. When the variance between two groups is the largest, the image is segmented with this gray value as the threshold. The specific algorithm is described as follows. Suppose an image has *m* points and the corresponding gray value is *n*, then the total pixel number can be calculated by:

$$\mathrm{N} = \sum_{i=1}^m n_i \tag{17}$$

The probability of gray value is defined as:

$$P_i = \frac{n_i}{N} \tag{18}$$

Then, parameter *k* is used to divide it into two groups $C_0 = [1\cdots k]$ and $C_1 = [k+1\cdots m]$, so the probability of C_0 group is described as:

$$\omega_0 = \frac{\sum_{i=1}^k n_i}{N} = \sum_{i=1}^k P_i \tag{19}$$

The probability of C_1 group is described as:

$$\omega_1 = \frac{\sum_{i=k+1}^m n_i}{N} = \sum_{i=k+1}^m P_i = 1 - \omega_0 \tag{20}$$

The average grayscale value of C_0 group is calculated by:

$$u_0 = \frac{\sum_{i=1}^k n_i * i}{\sum_{i=1}^k n_i} = \frac{\sum_{i=1}^m P_i * i}{\omega_0} \tag{21}$$

The average grayscale value of C_1 group is calculated by:

$$u_1 = \frac{\sum_{i=k+1}^m n_i * i}{\sum_{i=k+1}^m n_i} = \frac{\sum_{i=k+1}^m P_i * i}{\omega_1} \tag{22}$$

The overall average grayscale value is calculated by:

$$\mathrm{u} = \sum_{i=1}^m P_i * i \tag{23}$$

When the threshold value is *k*, the average value of gray is calculated by:

$$\mathrm{u}(k) = \sum_{i=1}^k P_i * i \tag{24}$$

The mean value of the sample gray values is $\mu = \omega_0 u_0 + \omega_1 u_0$. The variance between two groups is calculated by:

$$\mathrm{d}(k) = \omega_0(u_0 - u)^2 + \omega_1(u - u_1)^2 \tag{25}$$

Substitute Eq. (23) into Eq. (25) to obtain:

$$\mathrm{d}(k) = \omega_0\omega_1(u_1 - u_2)^2 \tag{26}$$

In this way, change k from 1 to m, and get k^* so as to satisfy $\mathrm{d}(k^*) = \max(d(k))$. Then, the image is segmented with the threshold k^*.

5. Expectation Maximization Algorithm

Expectation maximization (EM) algorithm is an iterative algorithm, which is used in statistics to find the maximum likelihood estimation of parameters in a probabilistic model dependent on unobserved recessive variables. This method can be widely used in the processing of defect data, truncated data, and other so-called incomplete data with noise. On the other hand. EM algorithm also can be used in the data clustering field of the machine learning and computer vision. The EM algorithm goes through the following steps.

Step 1: Calculate expectation *E.* Use the existed estimate of the probability model parameter to calculate the expectation of hidden variables. This step is named as Step E.

Step 2: Maximize *M.* Use the expectation of hidden variables obtained in Step 1 to carry out the maximum likelihood estimation of the model parameters. This step is named as Step M.

Step 3: The estimated parameters obtained in Step 2 are used in the calculation of Step 1, and then Step 1 and 2 are repeated alternately.

The mathematical model of EM algorithm is described as follows. Assume that the set $\mathrm{z} = (x,y)$ consists of the observed data x and unobserved data y. x and $\mathrm{z} = (x,y)$ are called the incomplete data and complete data respectively. Suppose the joint probability density of z is parameterized and defined as $\mathrm{p}(x,y|\theta)$, where θ represents the parameters to be estimated. The maximum likelihood estimation of θ is obtained by finding the maximum of logarithmic likelihood function $\mathrm{L}(x;\theta)$ on the incomplete data.

$$\mathrm{L}(x;\theta) = \log p(x|\theta) = \int p(x,y|\theta)dy \tag{27}$$

Based on the above descriptions, the specific algorithm steps are described as follows.

Input: observation data $\mathrm{x} = \left(x^{(1)},x^{(2)},\cdots,x^{(m)}\right)$, joint distribution $\mathrm{p}(x,z|\theta)$, conditional distribution $\mathrm{p}(z|x,\theta)$, and the maximum iteration number J.

Output: the model parameter θ.

(1) Randomly initialize the initial value θ^0 of model parameter θ.

(2) For j from 1 to J, start the following iteration process for EM algorithm:

(a) Step E: Calculate the conditional probability expectation of the joint distribution:

$$Q_i\left(z^{(i)}\right) = P\left(z^{(i)}|x^{(i)},\theta^j\right) \tag{28}$$

$$\mathrm{L}\left(\theta,\ \theta^j\right) = \sum_{i=1}^{m}\sum_{z^{(i)}} Q_i\left(z^{(i)}\right)\log P\left(x^{(i)},z^{(i)}|\theta\right) \tag{29}$$

(b) Step M: Maximize $\mathrm{L}\left(\theta,\ \theta^j\right)$ and get θ^{j+1}:

$$\theta^{j+1} = \arg\max_{\theta} L(\theta,\theta^j) \tag{30}$$

(c) If θ^{j+1j} reaches the convergence, the algorithm ends. Otherwise, return Step (a) for the iteration of Step E.

According to the judgment method of convergence, EM algorithm can guarantee to convergent to a stable point, but it cannot guarantee the convergence to the global maximum point, so it is a partial optimal algorithm. But when the optimization object $\mathrm{L}(\theta,\theta^j)$ is convex, EM algorithm can guarantee the convergence to the global maximum.

6. K-means Clustering Algorithm

K-mean clustering algorithm tries to divide the data into n groups of independent data samples, and make the variance among n groups clusters equal. The disadvantage of this algorithm is that it needs to determine the number of classes n in advance. Although some prepossessing algorithms can determine the value of n, it still increase a large part of the computational complexity. The following specific procedure is illustrated on this algorithm.

Step 1: Select the initial value μ_k of K centers.

Step 2: Classify each data point into the cluster with its closest central point.

Step 3: Substitute it into the following equation:

$$\mu_k = \frac{1}{N_k}\sum_{j\in cluster} x_j \tag{31}$$

Step 4: Repeat Step 2 until reach the maximum iteration number or the value of J less than a predetermined threshold.

7. Fuzzy C-Means Clustering Algorithm

Fuzzy C-means (FCM) clustering algorithm is an unsupervised fuzzy clustering method based on the optimization of a preset objective function, which is derived from the K-means clustering algorithm. The result of clustering is the membership degree of each data point to the cluster center expressed by a numerical value. It requires no human intervention in the process of algorithm implementation. The implementation principle of FCM clustering algorithm can be described as follows.

The objective function of the general fuzzy clustering analysis can be defined as:

$$J_m(U,P) = \sum_{i=1}^{c}\sum_{x_k\in X}(\mu_{ik})^m(d_{ik})^2\ s.t.U \in E_f \tag{32}$$

where, U is the original matrix, P is the clustering center, and d_{ik} represents the similarity between the sample point x_k and the i-th sample prototype P_i. Generally, the distance between two samples is expressed as a matrix norm, which can be expressed as the follows.

$$d_{ik}^2 = \| x_k - P_i\|_A = (x_k - P_i)^T A(x_k - P_i) \tag{33}$$

where, A represents the weight.

In order to achieve the optimal solution of the objective function of fuzzy clustering, the criterion of clustering can be set, that is to $\min\left\{\mathrm{J_m}\left(\mathrm{U},\ \mathrm{P}\right)\right\}$ under the constraint condition $\sum_{i=1}^{c}\mu_{ik} = 1$. Namely:

$$\min\left\{J_m\left(U,\ \mathrm{P}\right)\right\} = \sum_{k=1}^{\mathrm{n}}\min\left\{\sum_{i=1}^{c}(\mu_{ik})^m(d_{ik})^2\right\} \tag{34}$$

Therefore, under the constraint condition of membership degree $\sum_{i=1}^{c}\mu_{ik} = 1$, solve the problem $\min\left(\sum_{i=1}^{c}(\mu_{ik})^m(d_{ik})^2\right)$. The Lagrange method can be adopted to solve this problem, whose procedure can be described as follows.

Set the Lagrangian function as $\mathrm{F} = \sum_{i=1}^{c}((\mu_{ik})^m(d_{ik})^2) + \lambda\left(\sum_{i=1}^{c}\mu_{ik} - 1\right)$, where λ is a parameter. According to the specific solving process of Lagrangian algorithm, obtain $\mu_{jt} = \frac{1}{\sum_{i=1}^{c}\left[\frac{d_{jt}}{d_{it}}\right]^{-\frac{2}{m-1}}}$.

For the solution of the clustering center, the partial derivative is carried out on the objective function, that is to say $\frac{\partial J_m(U,P)}{\partial P_i} = 0$. So, the clustering center can be represented as $P_i = \frac{\sum_{k=1}^{n}(\mu_{ik})^m x_k}{\sum_{k=1}^{n}(\mu_{ik})^m}$.

The specific implementation steps of FCM algorithm can be described as follows.

Step 1: Randomly initialize the partition matrix U, clustering center P_i, and the distance norm d_{ik}.

Step 2: Calculate the cluster center P_i..

Step 3: Update the partition matrix U.

Step 4: Judge whether the iteration condition is satisfied. If it is satisfied, the iteration is terminated. Otherwise jump to Step 2 and continue to the iteration process until the termination condition is satisfied.

III. SIMULATION AND RESULT ANALYSIS

In order to analyze the performance of different segmentation algorithms on MRI images, seven typical segmentation algorithms were selected for carry out the simulation experiments. In order to show the obvious phenomenon, several typical MRI images (MRIs) were selected for experimental study, and the performance comparison results were obtained.

A. *Single-Tissue MRI Image Segmentation*

The MRI images stored in the format of BMP files with the size 60*60 are selected for the simulation experiments. The specific image is shown in Fig. 1 and Fig. 2 shows the histogram of the gray distribution for the MRI image. Fig. 3 shows the distribution of black and white images after each segmentation algorithm. The white part is the part separately segmented, and the black part is the reserved part. Fig. 4 shows the actual segmentation range of image segmentation after adopting each segmentation algorithm, where the blue line shows the ideal segmentation range and the red line shows the actual segmentation range.

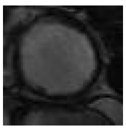

Fig. 1 MRI of brain tissue.

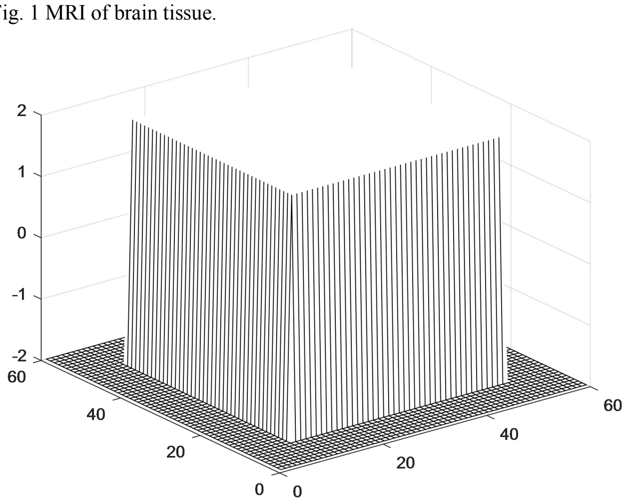

Fig. 2 Histogram graph of gray distribution.

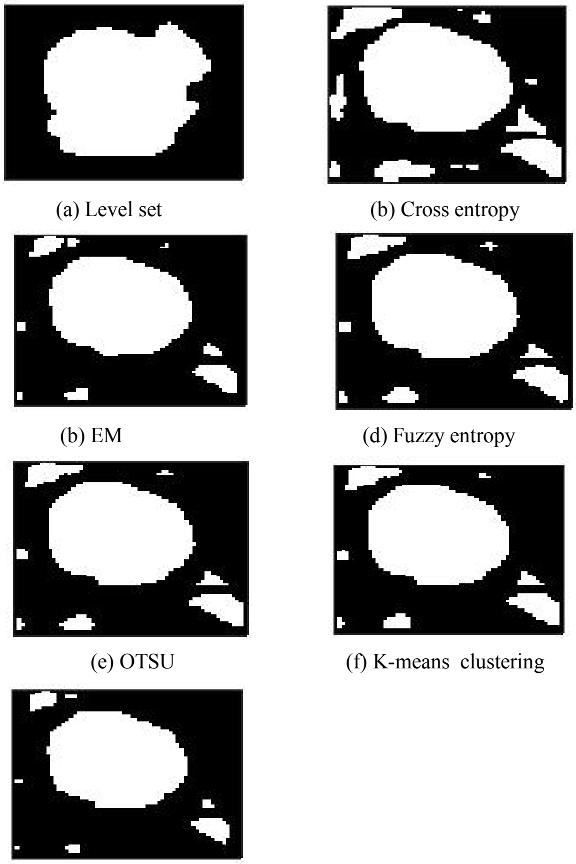

(a) Level set (b) Cross entropy

(b) EM (d) Fuzzy entropy

(e) OTSU (f) K-means clustering

(g) FCM

Fig. 3 The segmented black and white distribution images.

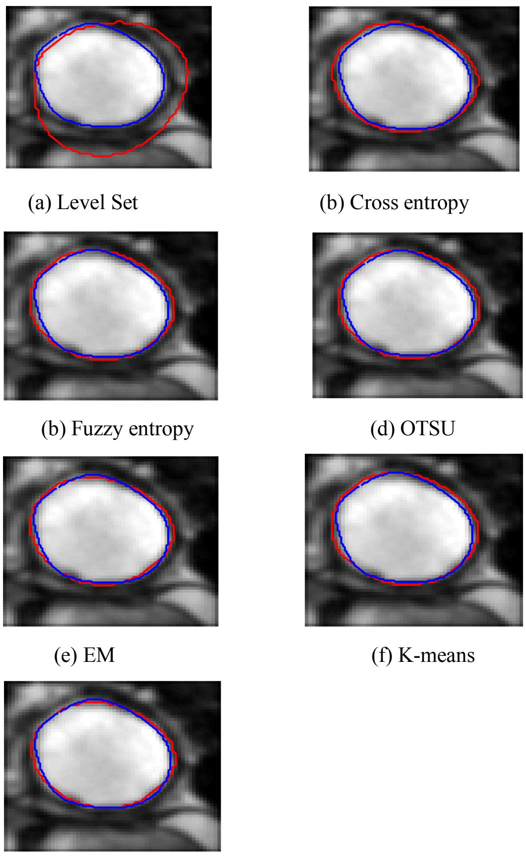

(a) Level Set (b) Cross entropy

(b) Fuzzy entropy (d) OTSU

(e) EM (f) K-means

(g) FCM

Fig. 4 Comparison results between actual segmentation effect and ideal segmentation effect.

It can be seen from the actual image segmentation results that for the single-tissue MRI segmentation all the other six algorithms have a good segmentation effect except the level set algorithm, and there is no big error. However, it does not mean that the level set algorithm is not a feasible segmentation algorithm.

B. *Brain MRI Image Segmentation*

The MRI stored in the format of PNG file and size of 528*528 is selected for the simulation experiments. The specific image is shown in Fig. 5, and Fig. 6 is the histogram graph of gray distribution of MRI. Fig. 7 shows the distribution of black and white images after each segmentation algorithm. The white part is the part separately segmented, and the black part is the reserved part. Fig. 8 shows the actual segmentation range of image segmentation after adopting each segmentation algorithm, where the red line shows the actual segmentation range.

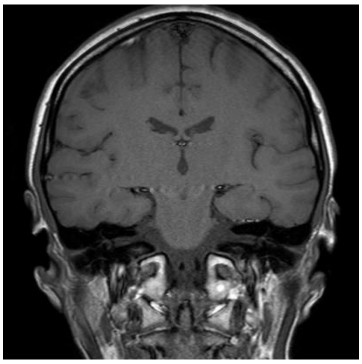

Fig. 5 Brain MRI.

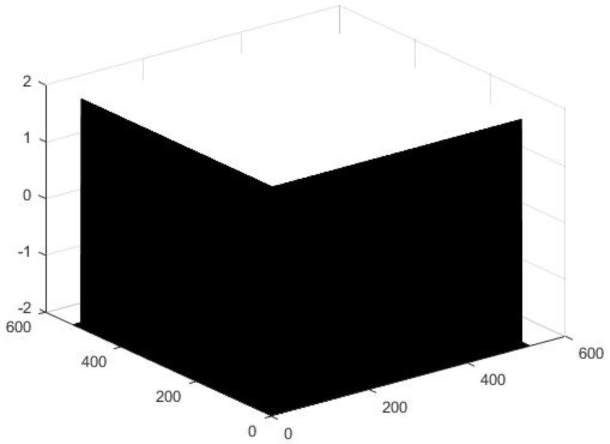

Fig.6 Histogram graph of gray distribution.

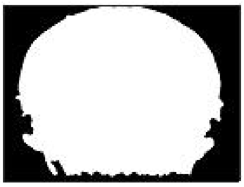

(a) Level set

(b) Cross entropy

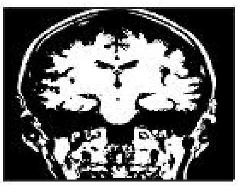

(c) Fuzzy entropy

(d) OTSU

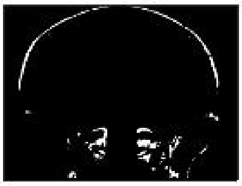

(e) EM

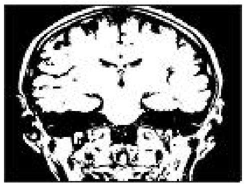

(f) K-means

(g) Fuzzy C-means

Fig. 7 The segmented black and white distribution images.

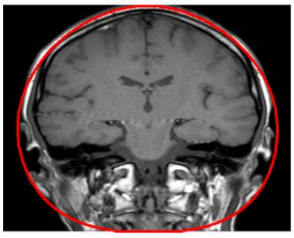

(a) Level Set

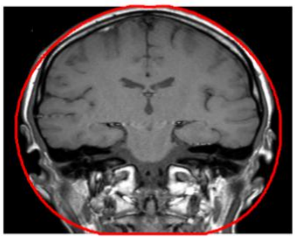

(b) Cross entropy

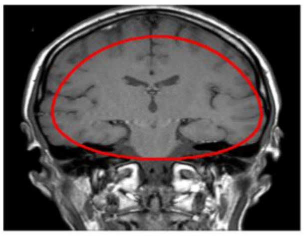

(c) Fuzzy entropy

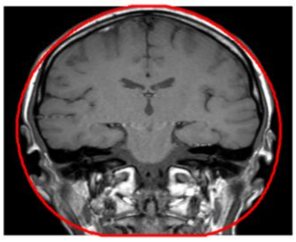

(d) OSTU

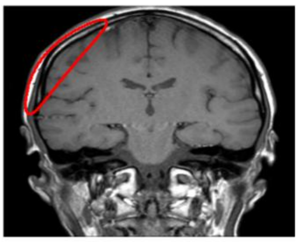

(e) EM

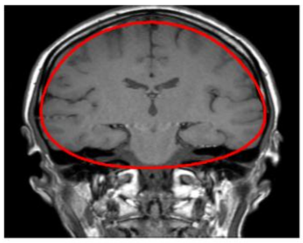

(f) K-means

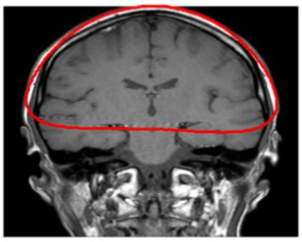

(g) FCM

Fig. 8 Actual segmentation ranges under each segmentation algorithm.

Seen from the results of the actual segmentation experiments, combined with the actual segmentation and segmentation distribution of black and white, each kind of segmentation algorithms corresponding whole brain MRIs, has its different regional segmentation and segmentation effect. For example, the fuzzy entropy algorithm is feasible for segmentation of brain internal parts of the segmentation. The segmentation of brain, cerebellum and other parts, and the specific segmentation of the edge should generally adopt the level set algorithm.

C. *MRI Image Segmentation of Abnormal Brain Tissue*

The MRIs stored in the format of JPG file and size of 256*256 are selected for the simulation experiments. The specific image is shown in Fig. 10, and Fig. 11 is the histogram graph of gray distribution of MRIs. Fig. 11 shows the distribution of black and white images after each segmentation algorithm. The white part is the part separately segmented, and the black part is the reserved part. Fig. 12 shows the actual segmentation range of image segmentation after adopting each segmentation algorithm, where the red line shows the actual segmentation range.

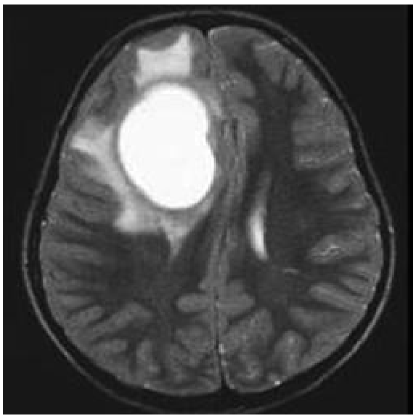

Fig. 9 MRI of brain cancer tissue.

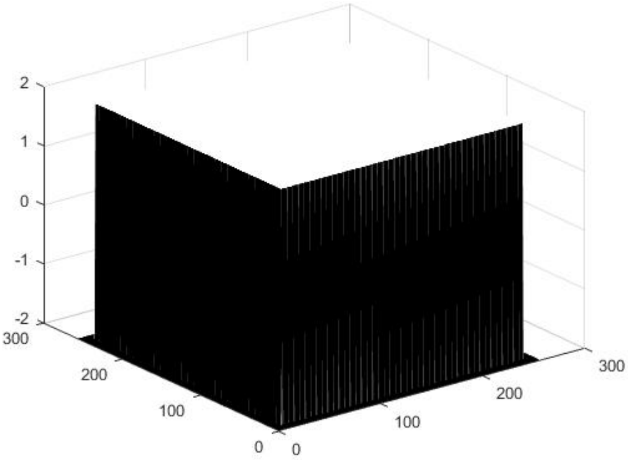

Fig. 10 Histogram graph of gray distribution.

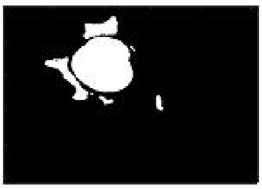

(a) Level set

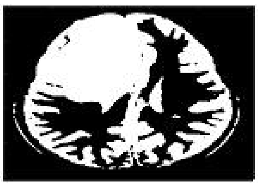

(b) Cross entropy

(c) Fuzzy entropy

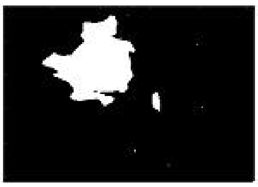

(d) OTSU

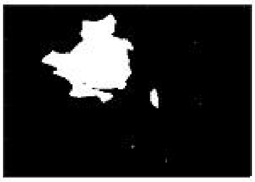

(e) EM

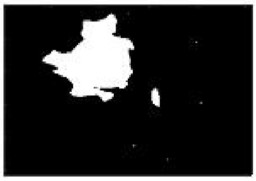

(f) K-means

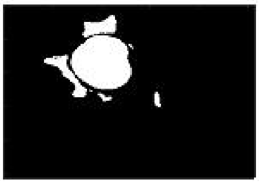

(g) FCM

Fig. 11 The segmented black and white distribution images.

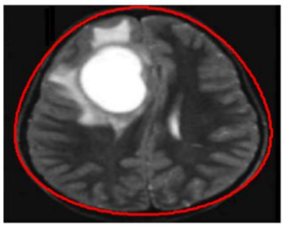

(a) Level Set

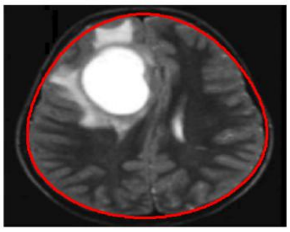

(b) Cross entropy

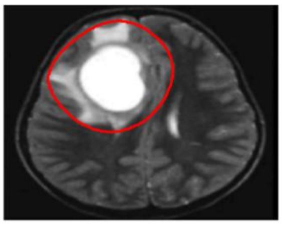

(c) Fuzzy entropy

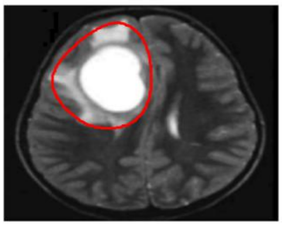

(d) OSTU

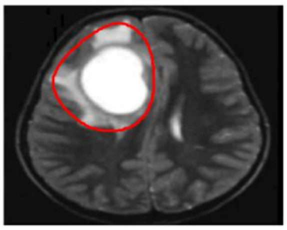

(e) EM

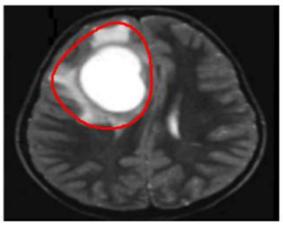

(f) K-means

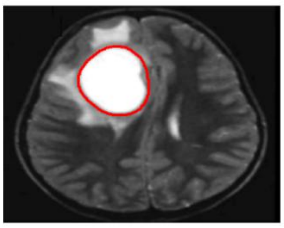

(g) FCM

Fig. 12 The segmented black and white distribution images.

Seen from the above actual segmentation effects and black and white distribution, there are certain differences among the algorithms for the segmentation of clinically abnormal tissues. It can be seen from the analysis of the actual simulation results that FCM clustering algorithm has a good segmentation effect. Other algorithms will have certain segmentation errors, where the level set algorithm and the cross-entropy based segmentation algorithm have a large deviation, but the application range of the algorithm is more suitable for edge segmentation, so the existence of deviation is also normal.

IV. CONCLUSIONS

In this paper, three types of MRIs are selected in different forms, and different image sizes and image file preservation formats. Seven segmentation methods are adopted to conduct image segmentation for different MRIs. It can be seen from the simulation results that each segmentation algorithm has its specific application range. For example, the level set algorithm is more suitable for the edge boundary segmentation of MRIs and the initial segmentation. The segmentation algorithm based on fuzzy entropy and the K-mean clustering algorithm are more suitable for the specific segmentation of the internal tissues of organs, and some aspects of tissue anatomy. On the whole, the FCM clustering algorithm, as a relatively advanced segmentation algorithm, has a good segmentation effect in various image segmentation aspects.

REFERENCES

[1] I. W. M. Wells, W. E. L. Grimson, R. Kikinis, and F. A. Jolesz, "Adaptive segmentation of MRI data," *IEEE Transactions on Medical Imaging*, vol. 15, no. 4, pp. 429-442, 1996.

[2] N. Mohd Saad, S. A. R. Abu-Bakar, Sobri Muda, M. Mokji, and A. R. Abdullah, "Fully automated region growing segmentation of brain lesion in diffusion-weighted MRI," *IAENG International Journal of Computer Science*, vol. 39, no. 2, pp. 155-164, 2012.

[3] M. A. Balafar, A. R. Ramli, M. I. Saripan, and S. Mashohor, "Review of brain MRI image segmentation methods," *Artificial Intelligence Review*, vol. 33, no. 3, pp. 261-274, 2010.

[4] S. Bricq, C. Ch, and J. P. Armspach, "Unifying framework for multimodal brain MRI segmentation based on Hidden Markov Chains," *Medical Image Analysis*, vol. 12, no. 6, pp. 639-652, 2008.

[5] H. Liu, H. Hu, X. Xu, and E. Song, "Automatic left ventricle segmentation in cardiac mri using topological stable-state thresholding and region restricted dynamic programming," *Academic Radiology*, vol. 19, no. 6, pp. 723-731, 2012.

[6] A. L. W. Bokde, S. J. Teipel, Y. Zebuhr, G. Leinsinger, L. Gootjes, and R. Schwarz, "A new rapid landmark-based regional MRI segmentation method of the brain," *Journal of the Neurological Sciences*, vol. 194, no. 1, pp. 35-40, 2002.

[7] A. R. Khan, L. Wang, and M. F. Beg, "FreeSurfer-initiated fully-automated subcortical brain segmentation in MRI using Large Deformation Diffeomorphic Metric Mapping," *Neuroimage*, vol. 41, no. 3, pp. 735-746, 2008.

[8] A. Pitiot, D. Hervé, P. Thompson, and N. Ayache, "Expert knowledge-guided segmentation system for brain MRI," *Neuroimage*, vol. Suppl 1, no. 1, pp. S85, 2004.

[9] L. Zhukov, K. Museth, D. E. Breen, A. H. Barr, and R. T. Whitaker, "Level set modeling and segmentation of diffusion tensor magnetic resonance imaging brain data," *Journal of Electronic Imaging*, vol. 12, no. 1, pp. 125-133, 2003.

[10] O. Colliot, T. Mansi, N, Bernasconi, "Segmentation of focal cortical dysplasia lesions on MRI using level set evolution," *Neuroimage*, vol. 32, no. 4, pp. 1621-1630, 2006.

[11] M. N. Ahmed, S. M. Yamany, N. Mohamed, A. A. Farag, and T. Moriarty, "A modified fuzzy C-means algorithm for bias field estimation and segmentation of MRI data," *IEEE Transactions on Medical Imaging*, vol. 21, no. 3, pp. 193-199, 2002.

[12] M. S. Yang, Y. J. Hu, C. R. Lin, and C. L. Lin, "Segmentation techniques for tissue differentiation in MRI of ophthalmology using fuzzy clustering algorithms," *Magnetic Resonance Imaging*, vol. 20, no. 2, pp. 173-179, 2002.

[13] Y. Nie, and P. F. Zhang, "Fuzzy partition and correlation for image segmentation with differential evolution," *IAENG International Journal of Computer Science*, vol. 40, no. 3, pp. 164-172, 2013.

[14] S. Pereira, A. Pinto, V. Alves, and C. A. Silva, "Brain tumor segmentation using convolutional neural networks in MRI images," *IEEE Transactions on Medical Imaging*, vol. 35, no. 5, pp. 1240-1251, 2016.

[15] A. Younis, M. Ibrahim, M. Kabuka, and N. John, "An artificial immune-activated neural network applied to brain 3D MRI segmentation," *Journal of Digital Imaging*, vol. 21, no. 1, pp. 69-88, 2008.

[16] Andrés Ortiz, Juan M. Górriz, Javier Ramírez, and Diego Salas-González, "Improving MRI segmentation with probabilistic GHSOM and multiobjective optimization," *Neurocomputing*, vol. 114, no. 11, pp. 118-131, 2013.

[17] X. Cui, L. Mili, G. Wang, and H. Yu, "Wavelet-based joint CT-MRI reconstruction," *Journal of X-ray Science and Technology*, vol. 26, no. 3, pp. 1-15, 2018.

Lin Chen is currently a master student in School of Electronic and Information Engineering, University of Science and Technology Liaoning, China. His main research interest is image processing and pattern recognition.

Dong Wei received his Ph. D. degree from Beihang University. He is currently an associate professor and Master's Supervisor in School of Electronic and Information Engineering, University of Science and Technology Liaoning. His main research interest is Computer Measurement and Control Technology.

Jie-Sheng Wang received his B. Sc. And M. Sc. degrees in control science from University of Science and Technology Liaoning, China in 1999 and 2002, respectively, and his Ph. D. degree in control science from Dalian University of Technology, China in 2006. He is currently a professor, Master's Supervisor and Doctoral Supervisor in School of Electronic and Information Engineering, University of Science and Technology Liaoning. His main research interest is modeling of complex industry process, intelligent control and Computer integrated manufacturing.